

Effects of muscle tense on impact responses of lower extremity

Takahiko Sugiyama, Hideyuki Kimpara, Masami Iwamoto, Daisuke Yamada,
Yuko Nakahira and Masatoshi Hada
TOYOTA Central R&D Labs., Inc.

ABSTRACT

This paper describes investigation on the effects of muscle tense in bracing on impact responses of driver's lower extremity in frontal impacts. From an experimental volunteer test data using a male subject, 33 muscle activation levels of right lower extremity for his maximal voluntary contraction in pressing on a brake pedal were predicted by a musculoskeletal model and then used for a human FE model. Parametric studies on pedal impacts to the foot with three pre-impact muscular conditions reveal that activated thigh muscles can increase axial compressive force and possibility of bone fractures at the tibia.

Keywords: Muscle activation, Finite Element Method, Musculoskeletal Model, Bracing, Lower extremity

MUSCLE ACTIVATION must be considered in the crashworthiness as an essential effect to biomechanical responses and occupant injuries. In case of approaching a crash, it is conjectured that vehicular occupants would brace themselves with activating their muscles. Tensed muscles may change occupant's posture and stiffen up their joint articulations, while occupant's posture and biomechanical apparent stiffness would determine impact responses of the human body. Therefore, it can be assumed that muscle tense affects injury patterns and severities as well as impact responses during automotive crashes.

Several studies have been performed to investigate the influence of muscle tense to the injuries. Tennyson and King (1976) conducted a series of neck loading cadaveric tests and reported that muscle tense increased the neck injury in higher acceleration, while muscle tense contributed to the decrease in neck injury probability in low acceleration. This study suggested inherent performance tradeoffs in the role of muscle tense on the injury severities in impact loadings. Begeman et al. (1980) conducted a series of sled test using human volunteers and cadaveric subjects and investigated the influence of muscle tense on kinematics of the lower extremities. Electromyogram (EMG) technology was used to identify muscular activities. As the results, they revealed that muscle tense stiffened up the human body rigidly and alter the overall kinematics of the human body during whole impact events. Funk et al. (2001) performed cadaveric axial impact tests for the foot and ankle complex under a condition to simulate entrapped knee. In their tests, a foot plate hit the foot axially with an initial velocity of 5 m/s while muscular tension forces of 0 kN, 1.7 kN or 2.6 kN were applied to the Achilles tendon for investigation of muscular effect to skeletal injuries of the lower leg. They found that the muscular tension force can increase axial compressive force and the possibility of bone fractures at the distal tibia. On the other hand, some benefit effects of muscle tense were also reported. Klopp et al. (1995) performed numerical simulation, pendulum tests and sled tests using dummies and cadavers to investigate muscular effect to occupant injuries. They concluded that muscular bracing of the legs acted as additional restraints and reduced horizontal pelvic motion. Levine et al. (1978) conducted frontal impact tests using cadavers restrained by a three-point belt system equipped with and without a knee brace which simulated muscular tense of quadriceps in thigh. They found that the knee brace played a role in the prevention of submarining in frontal collisions. Therefore, the muscle tense appears to have both aspects of advantage and disadvantage for occupant injuries. However, it is not fully understood how muscle tense affects the impact responses and injury severities.

This study particularly focused on the lower extremity of vehicular occupants, because the lower extremity is the second most commonly injured body part for vehicular occupants (States, 1986; Morgan et al., 1991). Additionally, some lower extremity injuries might cause long term disability and impairment (States, 1986), while those are not fatal ones. Morgan et al. (1991) estimated that pedal interaction was the major cause of foot and ankle injuries based on NASS database. Their

analysis showed that 57 % of the drivers who sustained moderate or greater ankle injuries were injured while the foot was on the pedal. However, there are no accident data to explain how the muscle tense in bracing affects the ankle injuries of drivers. Finite Element Method (FEM) simulations using human body models with and without muscle activation have the possibility to investigate the muscular effects.

A great number of finite element (FE) models of human body has been developed and validated against cadaveric experimental data. Although few studies (e.g. Camacho, et al., 1997) attempted to validate them for volunteer subjects with muscle tense, most of FE studies could not indicate the effects of muscle tense on impact responses and injuries due to limitations of FE techniques. Recently, Choi et al. (2005) conducted both of sled tests using eight volunteer subjects and computational analysis using a human FE model in frontal impact. They used the EMG as an indicator of muscle activation levels and normalized it against that of maximal voluntary contraction. Reaction forces on steering wheel and brake pedal predicted by using their FE model with 16 muscles in the upper and lower extremities agreed with those of experimental data. However, due to the definition of joint model, bone fractures on the articulated joints or ligamentous injuries could not be predicted in their model. In addition, muscles in deep layers were not considered in the motion analysis of the human body. Behr et al. (2006) developed a FE model of the lower limb with 20 independent muscle bundles in the superficial and deep layers and used to investigate the effect of muscle tense on the skeletal injuries of the lower limb. They found that muscle activation in a frontal impact loading condition significantly increased the stress level on the tibial shaft. Since their model did not include muscles of the foot and hip, however, the model was not enough to reproduce driver's bracing in an emergency braking.

The aim of this study is to determine how the muscle tense affects the impact responses and injury severities of the lower extremities. To achieve the research object, this study conducted an experimental test using a volunteer subject, computational analysis using a musculoskeletal model, and parametric simulations using FE human model.

METHODS

This study concentrated research objects on a pedal impact to the driver's sole of the foot during pressing on the brake. To achieve our research goals, four research steps were conducted in this study: (1) experimental study using a human volunteer, (2) prediction of muscle activation levels from obtained experimental data by using a 3D musculoskeletal model, (3) reconstruction of the volunteer's bracing condition using a 3D FE human model, and (4) parametric study for pre-impact muscular conditions. Detailed explanations are expressed in the following sections.

EXPERIMENTAL STUDY: An experimental system (Figure 1) was developed in order to obtain 3D motion, reaction forces, and muscle activation levels of the subject's right lower extremities during pressing on the brake. A flexible driving position system (FDPS) provided a vehicular driving environment. All positions and angles of FDPS including a rigid seat bottom, rigid seatback, steering handle, and brake pedal were adjusted to provide a volunteer subject's usual driving posture. A 3D motion analysis system (Eagle/Hawk digital system, Motion Analysis, USA) was used to capture a motion of human body and a part of FDPS segments. Reflective markers were placed on the subject's pelvis, right lower extremity, and surface of FDPS in order to identify their kinematics. To identify translational and rotational positions of body segments in the global coordinate system, each segment had the local coordinates using a group of three or more markers. Seventeen and fourteen markers were used for the test subject and FDPS, respectively. At the same time, pedal force, reaction forces on the steering handle, muscle activities of lower extremity, and pressure distributions on a flat rigid seat back and bottom were measured using a three-axis load cell (9602A, Kistler, Germany), high impedance load cell (9212, Kistler, Germany), an EMG measurement system (MP150, Biopac systems, USA), and a seat sensor (BigMat, Nitta, Japan), respectively. Motion data were captured at a sampling rate of 100 Hz. The pedal force, reaction force on the steering handle, and EMG were sampled at 1 kHz and then EMG data were filtered using a low pass filter of 500 Hz. However, due to limitation of sampling rates, pressure distribution of the seat sensor was sampled at 100 Hz. A single trigger pulse synchronized all measurement systems.

A 31 years old human male volunteer who had a height of 1.77 m and a weight of 75 kg, which were similar as those of a mid-size male (American Male 50th percentile: AM50), was employed for

this study. Preliminarily, the EMG of maximum voluntary contraction for all 10 muscles (Figure 2) was measured and integrated to obtain maximum Integrated rectified EMG ($IEMG_{max}$). Then, the test subject was asked to do the following task. Firstly, the subject was seated on the rigid seat and asked to be relaxed. At this moment, subject's foot was placed on the brake. Then, the subject braced his whole body and pressed the brake pedal using the right lower extremity with maximal voluntary force. The brake pedal was fixed against FDPS, so that the pedal angle was not changed during the pedal operation. Upper torso of the subject was firmly fixed on the rigid seat back by braced upper extremity. This term is called bracing period. Secondary, the pressing force was maintained for one second. This term is maximum voluntary contraction period. Thirdly, the subject was asked to release the force of the right lower extremity, which is called relaxing period. All motions were completed within four seconds. Integrated rectified EMG (IEMG) was estimated from all EMG data. Pre-measured $IEMG_{max}$ was used for normalization of measured IEMG data. The normalized IEMG was assumed to be muscle activation level in this study.

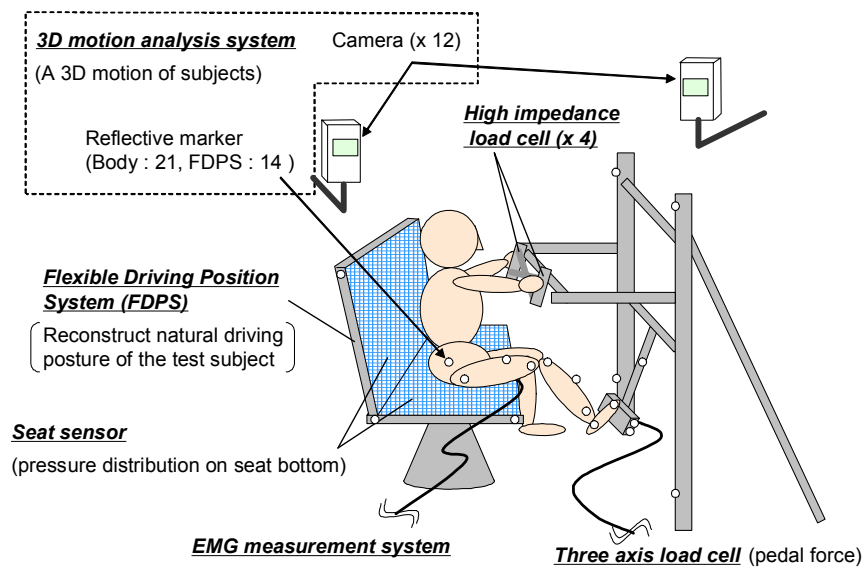


Figure 1: Diagram of experimental environment

MUSCULOSKELETAL MODEL: A musculoskeletal model (Hada et al., 2007) was used to predict muscle activation levels of the lower extremity during pressing on the brake. The advantage of using this musculoskeletal model was ability to calculate muscle activities in deep layer as well as those in superficial layer, while EMG technology can estimate muscle activities in only superficial layer. Figure 2 describes the musculoskeletal model of right lower extremity, which consisted of four rigid body segments of pelvis, femur, tibia/fibula, and foot. Each segment length was matched with that of a commercially available human FE model, THUMS-AM50 (Iwamoto et al., 2002). All body segments were linked with three articulated joints of the hip, knee, and ankle. The relaxed zero-G posture of human body (Griffin, 1978) was assumed as the optimal posture for muscles in this study. Muscles were modeled with a Hill-type (Winters, 1990) 1D bar element. Muscle i contraction force f_m^i in the Hill-type muscle is generally defined as follows:

$$f_m^i = a^i \cdot f_{max}^i \cdot f_l(l_m^i) \cdot f_v(l_m^i, \dot{l}_m^i) + f_{max}^i \cdot f_p(l_m^i) \quad (1)$$

where the variable a^i represents an activation level of muscle which is in range from 0 to 1. The constant f_{max}^i stands for a maximum contraction force of muscle i , which is determined by the constant variable of maximum contraction force per unit cross-sectional area multiplied by physiological cross section area (PCSA) of skeletal muscle i . Gans (1982) reported the maximum contraction force per unit cross-sectional area was 5.5 kgf/cm^2 . Winters (1990) summarized PCSA

of all skeletal muscles. The functions of $f_l(l_m^i)$, $f_v(l_m^i, \dot{l}_m^i)$, and $f_p(l_m^i)$ are defined as active force-length, active force-velocity, and passive force-length relations of muscle. However, these functions were simplified as $f_l \equiv 1$, $f_v \equiv 1$, and $f_p \equiv 0$ in this study. Since the posture of lower extremities at the bracing period was similar to the optimal posture, the changes of muscle lengths would be less than 10%, which was estimated by musculoskeletal model. Considering the non-linear shapes of f_l and f_p curves (Lloyd and Beiser, 2003), the variables of f_l and f_p would be relatively equal to 1 and 0, respectively. Additionally, the posture of the lower extremities was fixed in braced boundary conditions, so that the f_v also can be simplified as 1.

In the musculoskeletal model, muscle forces were assumed to work only for a contraction of muscle segment in its axial dimension. The muscle attachments to the bones were represented as centroidal points of origin and insertions. Via-points were also inserted to form reasonable muscle-paths. Since some large attachment areas, such as series of gluteus and adductor magnus, had multi-purposes for their function, the attachments included several 1D bar elements to form multi-muscle-paths. Consequently, 33 skeletal muscles (modeled by 41 bar elements) on right lower extremity were modeled in this study.

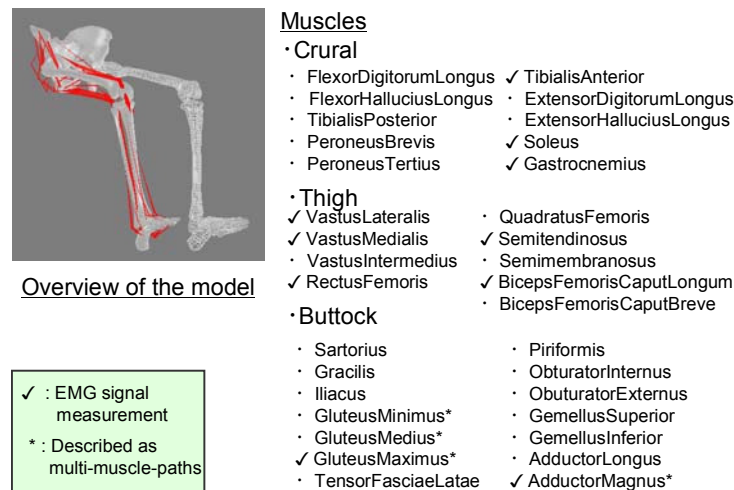


Figure 2: Musculoskeletal model and list of muscles considered in this study

The relationship between muscle force F_m and joint torque τ is described mathematically by the Jacobian \mathbf{J}_m :

$$\tau = -\mathbf{J}_m^T F_m \quad (2)$$

where F_m is muscle force vector which includes all muscles force elements. According to the virtual work principle, equation (2) can be described as follows:

$$\Delta l_m = \mathbf{J}_m \Delta \theta_j \quad (3)$$

where Δl_m is length changes of muscle, and $\Delta \theta_j$ is angle changes of joint. The Jacobian \mathbf{J}_m plays a role of muscle moment arm and replaces joint torque with muscle force. In this study, twenty-three moment arms of all 33 skeletal muscles were validated against those of experimental data (e.g. Spoor et al., 1990; Buford et al., 1997).

INVERSE DYNAMICS: Several calculation steps of inverse dynamics analysis using the musculoskeletal model were performed to estimate muscle activation levels from volunteer test data. Firstly, 3D motion and external forces obtained from the experimental data were used to estimate the joint torques of all body articulations. The following equation of motion, which was described as a

function of joint angle vector $q(t)$, was used to determine joint torques τ of all joints:

$$M(q)\ddot{q} + h(q, \dot{q}) + g(q) = \tau - J_e^T F_e \quad (4)$$

where the variables of $\dot{q}(t)$ and $\ddot{q}(t)$ are angular vectors of joint velocity and acceleration, respectively. The functions of M , h , and g represent an inertia matrix, centrifugal and coriolis force term, and a gravity force term, respectively. The symbols of F_e , and J_e stand for external forces and Jacobian matrix for external forces, respectively. The boundary condition of the musculoskeletal model was assumed that effect of upper body forces could be replaced with the fixed pelvis in this study. The fixed pelvis caused associated forces and moments at the hip joints in solving the inverse dynamics problem.

Secondary, obtained joint torque τ from equation (4) was assigned to muscle forces based on the equation (2). Since the number of muscles was generally greater than degrees of freedom of articulated joints, an optimization method is required to determine the muscle forces. This study assumed the principal of minimal total squared non-dimensional muscle force. The objective function $E(F_m)$ for optimization is defined as follows:

$$E(F_m) = F_m^T W^T W F_m \quad (5)$$

The tensor of W is a diagonal matrix of weighting factor and defined as follows:

$$W = \text{diag}\{1/k\rho_i\} \quad (6)$$

where the constant k is coefficient which represents muscle force per unit area, and constant ρ_i is PCSA of muscle i .

Finally, muscle activation level was obtained as a ratio of estimated muscle force against the maximum voluntary contraction force. In this study, the predicted muscle activation levels at a moment of pressing on the brake were used as inputs for a FE human model. More detailed descriptions for the musculoskeletal model and inverse dynamics are reported in the previous reports (Hada et al., 2007; Yamada and Hada, 2007).

VALIDATION FOR PREDICTED MUSCLE ACTIVATION LEVELS: Yamada and Hada (2007) reported on a validation of the musculoskeletal model used in this study. In their report, another series of volunteer test using three subjects was conducted to estimate the normalized IEMG. Additionally, the subjects performed braking motion in three different ankle joint rotated conditions. As the result, the pattern of normalized IEMG, predicted muscle activation levels of each subjects, and postures were well matched together.

HUMAN FE MODEL: A commercially available mid-sized human male occupant model THUMS-AM50 (Version 1.61, Toyota Central R&D Labs., Inc.; Iwamoto et al., 2002) was used with some modifications of geometry and FE mesh of the lower extremity. The cortical bone of lower extremity was represented by the elastic plastic solid elements. The material properties were determined from the previous report (Iwamoto et al., 2005). The yield stress of 95.4 MPa and ultimate plastic strain of 2.0% were assumed for cortical bone of the tibia. The hip and knee articulations were assumed as a rotational joint, however, ankle articulation was modeled as bone-to-bone contacts without joint definition and the joint stiffness was controlled by major ligaments. Thirty-three muscle models considered in the musculoskeletal model were duplicated in the FE model as shown in Figure 3. The material model for muscles used in LS-DYNA was *MAT_MUSCLE (LS-DYNA Material Type 156) based on the Hill-type muscle law as described in equation (1). The maximum contraction force was determined from the literature (Winters, 1990 and Gans, 1982). Although most of assumed parameters for muscles in the human FE model were comparable to those of the musculoskeletal model, passive tensile property of the muscles obtained from the literature (Yamada, 1970) was added to the muscle models in the human FE model. Additionally, the definition of *CONTACT_GUIDED_CABLE was used for the representation of via-points.

PARAMETRIC STUDY ON PEDAL IMPACTS: Before performing parametric study, some preparations for the human FE model were conducted. Firstly, the posture of the right lower extremity was modified to make the same posture as the volunteer subject pressed on the brake pedal with his maximal voluntary contraction in the test (Figure 4). In contrary, upper bodies and left lower extremity were kept in default posture of THUMS because 3D motions of those parts were not

captured. Secondly, pressure distributions on the seat bottom were calculated using the modified human FE model and compared with those obtained from the volunteer test to reproduce the volunteer test condition. In this study, muscles were represented as a 1D bar element, which can simulate only for contractional direction force. However, the effect of muscular volume and stiffness changes could not be represented in the lower extremity model. Therefore, this study compared the patterns of pressure distribution at the moment before bracing. Then, the model posture was slightly modified to fit the posture of bracing period.

A series of parametric study was then performed to investigate the effects of muscles on impact responses to the sole of foot. Figure 5 illustrates a simulation setup of this parametric study. A rigid impactor was used to apply a dynamic external force on the sole of foot in the anteroposterior direction. The impactor had a rectangular solid shape imitating a brake pedal with a mass of 30 kg and a velocity of 5.0 m/s. Three FE models were prepared: (1) with activated muscles, (2) with relaxed muscles, and (3) without any muscle of lower extremity. The muscle activation levels used for FE model were obtained from predicted variables by the musculoskeletal model. All simulation series were done using a commercially available FE solver, LS-DYNA 971 revision 7600.398 (LSTC, Livermore, CA) on an Intel Xeon 64 bit based computer.

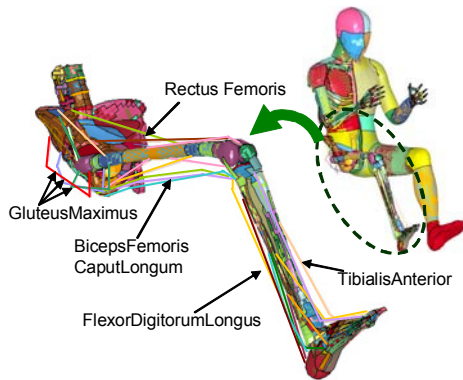


Figure 3: Thirty-three muscles on a FE human model of lower extremity

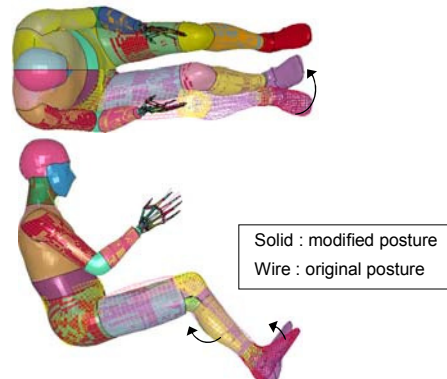


Figure 4: Top and lateral views of posture modification

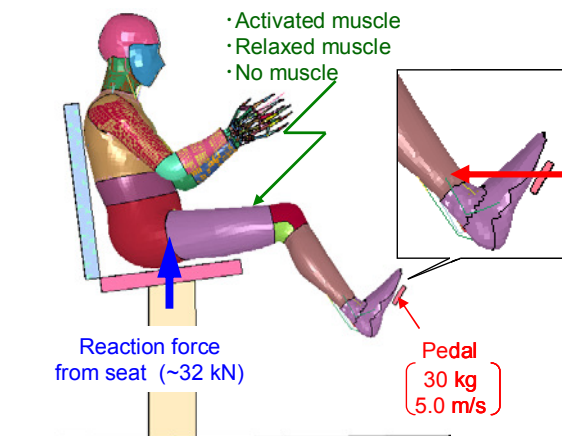


Figure 5: Simulation setup for parametric study on impacts to the sole of foot

INJURY PREDICTORS: This study employed two injury predictors for skeletal injuries; plastic strain and the Revised Tibia Index (RTI). In the FE analysis of this study, the bone elements were assumed to be mechanically damaged when the stress reached yield threshold of 95.4 MPa (Iwamoto et al, 2005). The FE analysis indicated the plastic strain at yielded bone elements. The

RTI (Kuppa et al., 2001) was described to suggest the probability of leg fracture (AIS 2+) as the following equation,

$$RTI = \frac{F}{240} + \frac{M}{12} \quad (7)$$

where the variable F is the measured compressive axial force (kN), the variable M is the resultant bending moment in the X and Y directions (Nm). According to risk curves proposed by Kuppa et al., (2001), the RTI values of 1.16, 1.0, and 0.91 correspond 25%, 33%, and 50% probability of the AIS 2+ leg injury.

RESULTS

MODEL VALIDATION: Predicted muscle activation levels for 10 major surface muscles (marked muscle names in Figure 2) using the musculoskeletal model were validated against measured normalized IEMG. Figure 6 indicates time history curves of vastus lateralis's and soleus's muscle activation level (dotted lines) and experimental result of normalized IEMG (solid lines) during pressing on the brake. These two muscles were selected as primal muscles in extension of knee joint and plantar flexion of ankle joint, respectively. The time history curves could be divided into bracing, maximal voluntary contraction, and relaxed terms. The model predictions are matched the experiment results reasonably well.

Figure 7 shows inferior views of pressure distributions on the seat bottom between those obtained experimentally (a) and predicted by the FE model (b). The front and right sides of subject were respectively described on right and superior sides of the Figure 7. The pattern of distribution was captured immediately prior to the brake motion. The highest pressure was observed around both iliac bones. The pressure distribution characteristics predicted by the model seemed to fit the experimental data reasonably. Additionally, the model predictions of contact forces (718 kN) on the seat bottom generally agreed with the experimental results (643 kN).

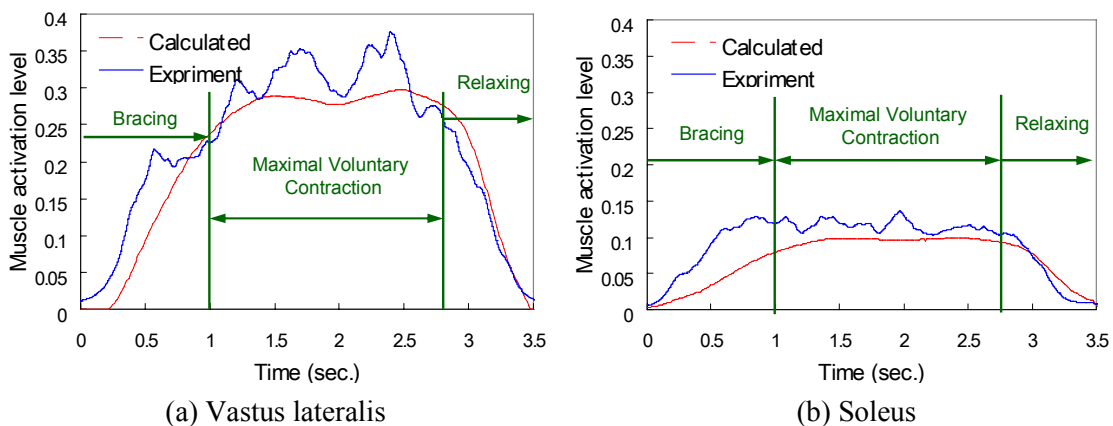
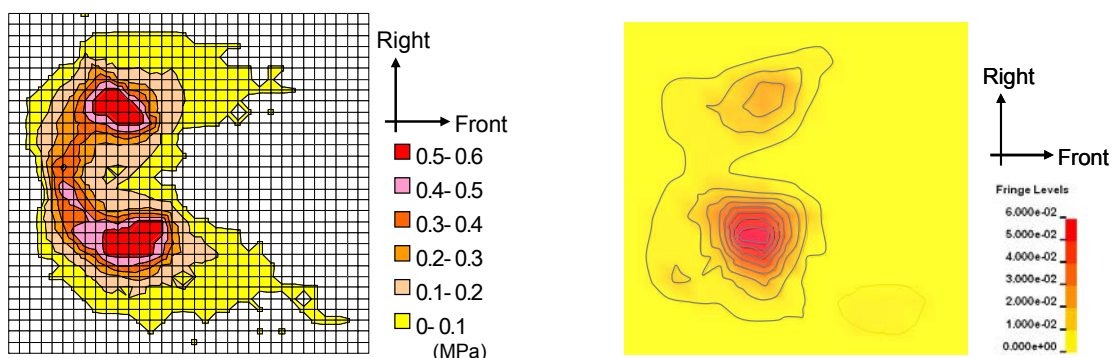


Figure 6: Typical muscle activated patterns



(a) Experimental

(b) FE analysis

Figure 7: Pressure distribution between a test subject and a seat bottom (inferior view)

The peak force on the brake pedal was 710 N in this study. This variable was comparable to previous reports; Owen et al. (1998) reported that the emergency braking force was ranged from 431 to 1150 N (4 male; Height, 1.72-1.76 m; Age, 20-50) using a driving simulator, while Yoshida (1998) reported 800 N of the brake pedal force.

ESTIMATED MUSCLE FORCES: Figure 8 shows predicted muscle forces contributing to flexion and extension of ankle, knee, and hip joints in activated and relaxed muscle conditions. Table 1 shows a list of major flexor and extensor muscles at each joint. Figure 9 indicates that plantar flexor muscle of the soleus attached to the Achilles tendon was significantly activated to press the brake pedal in the activated case. In addition, extensor muscles of vastus lateralis and gluteus maximus at the knee and hip joints were activated as well as flexor muscle of biceps femoris at the knee joint was activated. Since forces of extensor muscles were greater than those of flexor muscles at both the knee and hip joints, the muscles in the hip and right thigh could contribute to the extension of the knee and hip joints in pressing the brake pedal. In the relaxed muscular condition, the flexor muscle generated force at the ankle joint while the extensor muscle generated force at the knee joint. However, the forces are much smaller than those predicted in the activated condition.

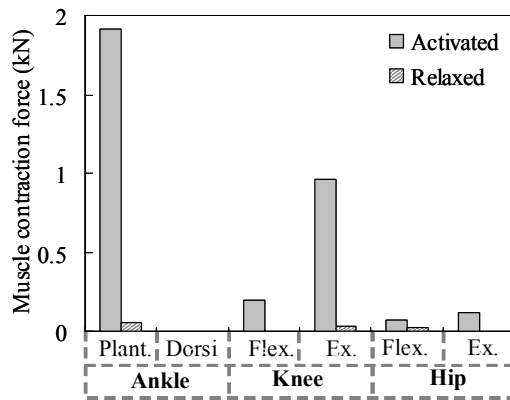
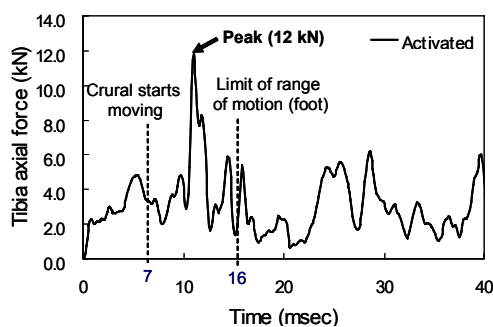


Table 1: List of major flexor and extensor muscles at each joint

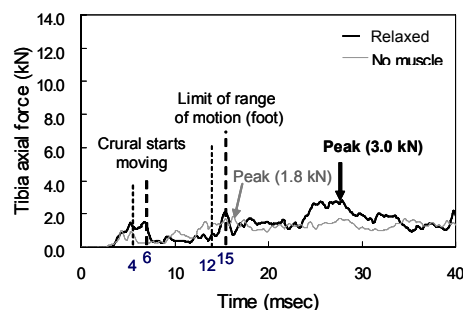
Joint	Type	Muscle	Location
Ankle	Plantar flexion	Soleus	Crural
	Dorsi flexion	Tibialis anterior	Crural
Knee	Flexion	Biceps femoris caput longum	Thigh
	Extension	Vastus lateralis	Thigh
Hip	Flexion	Rectus femoris	Buttock
	Extension	Gluteus maximus	Buttock

Figure 8: Muscle forces for flexion/extension at Each joint in activated and relaxed conditions

PARAMETRIC STUDY ON PEDAL IMPACTS: Figure 9 describes a comparison of axial compressive forces on the tibia predicted by the FE model among several muscle conditions; the case with activated muscle was described on graph (a), the cases of relaxed muscle and no muscle were indicated by solid and gray lines on graph (b), respectively. The peak compressive force of 12 kN in activated muscle was significantly greater than that in relaxed muscle or no muscle cases. The peak compressive force in relaxed muscle case was relatively greater than that in no muscle case.



(a) Activated muscle case



(b) Relaxed muscle and no muscle cases

Figure 9: Comparison of the applied force to the tibia

INJURY PROBABILITY: Figure 10 represents contour diagrams of plastic strain on the tibia. It is found the different patterns of plastic strain between muscle activated and non-activated cases. The concentrated plastic strain was observed at the diaphysis of the tibia and the medial malleolus in muscle activated, while the muscle relaxed case had plastic strain at anterior surface for the talus. However, no plastic strain was observed in the case of no muscle model. The areas of yielded FE elements in the activated and relaxed cases were 748 mm³ and 574 mm³, respectively.

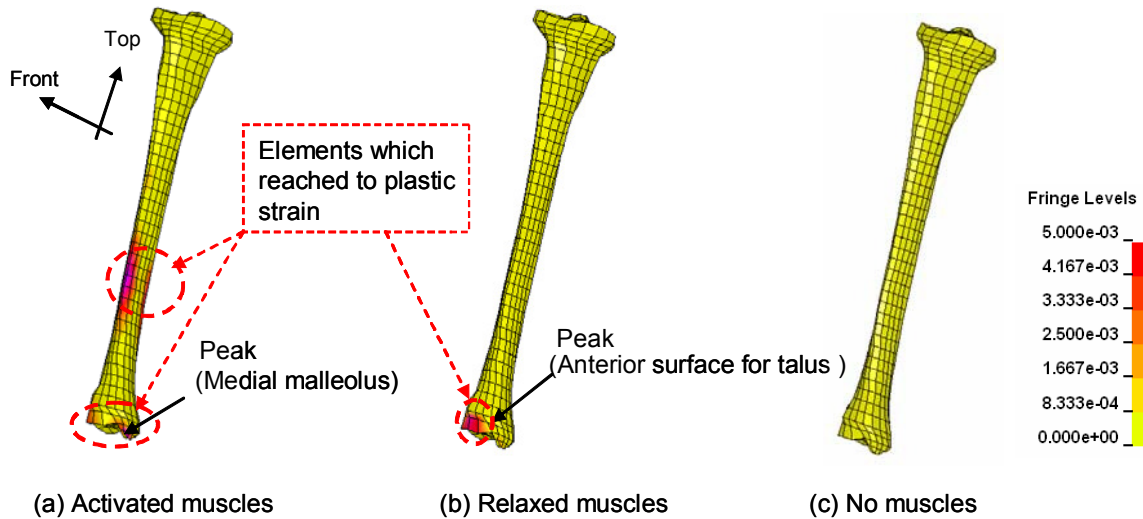


Figure 10: Oblique views (frontal left) of plastic strain distributions on right tibia bone

Figure 11 shows the time history curves of the RTI at the diaphysis and distal end of tibia. The RTI value of the diaphysis in activated muscle case indicated the greatest peak, which was beyond the threshold of 50% probability of AIS 2+ leg injury. However, the other cases could not reach 25% probability level of the RTI value.

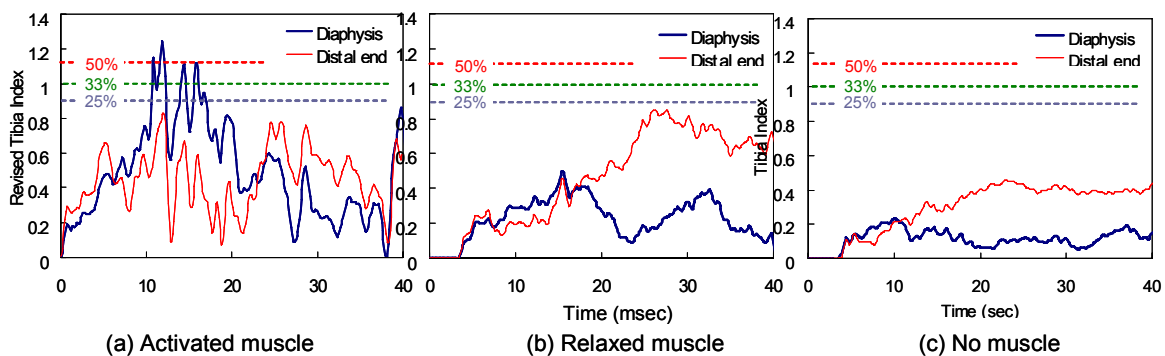


Figure 11: Comparison of the Revised Tibia Index value

DISCUSSION

Computer simulations using a human FE model were performed to investigate effect of muscle tense caused by drivers' bracing before impacts on skeletal injuries of the lower leg. A preliminary volunteer test was conducted to reproduce one of the bracing conditions in drivers' braking motions. Since it was difficult to reproduce real muscle reaction of a driver in an emergency braking at the

laboratory test, however, a 31 years old male subject, who was similar to the body size of AM50 and had 11 years experience as a driver, was asked to press a brake pedal by his right leg with his maximal voluntary contraction in this study. Although it is still unknown if a driver can yield the maximal voluntary contraction in an emergency braking before impact, in this study, this particular test condition was used to investigate effect of muscle tense in bracing on the lower leg skeletal injury of a driver similar to AM50.

Based on the measurements obtained from the volunteer test, in this study, activation level of each muscle was estimated by using a musculoskeletal model which could simulate 33 skeletal muscles of the right lower extremity including deep layer as well as superficial layer. In previous studies using cadaver tests and computer simulations, only an Achilles tendon force or muscular forces contributing to flexion of the ankle joint were considered to investigate the muscular effects for the lower leg skeletal injuries (e.g. Funk et al., 2001 and Kitagawa et al., 1998). However, each muscle collaboratively works with the other muscles during a human motion. Therefore, several muscles of the lower extremity can work together in a braking motion. In our previous work, we conducted a series of volunteer tests using three male subjects to measure activation level of each muscle in the lower extremity during pressing a pedal. We found that some muscles other than the soleus and gastrocnemial muscle contributing to flexion of the ankle joint were activated in the motion (Hada et al., 2007). Thus, it is critical to simulate activation levels of all the related muscles to the braking motion in the lower extremity.

The interaction forces between upper extremity and steering handle as well as forces from the seat back could affect prediction of muscular activation levels in solving the inverse dynamics problem. Actually, we measured the interaction forces between the hands and a steering handle and forces from the seat back in addition to forces from the seat bottom and the pedal force. As a result, these external forces and muscular forces of whole body worked together and kept the pelvis fixed during the bracing period. In this study, we focused on the muscular effects of the lower extremity on the skeletal injuries. Therefore, we simplified the boundary condition of the musculoskeletal model and assumed that effect of upper body forces could be replaced with the fixed pelvis. The fixed pelvis caused associated forces and moments at the hip joints in solving the inverse dynamics problem. This is a first approximation used for application of the lower extremity musculoskeletal model to occupant injury prediction. Further studies are needed to develop musculoskeletal models of upper bodies and apply the models to occupant injury prediction.

In previous study performed by Yamada and Hada (2007), the same musculoskeletal model and optimization method used in this study was used to predict activation levels of each muscle in the right lower extremity. In their study, three volunteers were employed and asked to press the brake pedal in three different ankle positions with internal rotation, fullface, and external rotation. Their study revealed that this musculoskeletal model and optimization method could predict activation level of each muscle accurately. In addition, activation levels of 10 muscles for the test subject predicted by the musculoskeletal model in this study showed good agreement with normalized IEMG obtained from the experimental volunteer test. The predicted activation levels can be assumed as those for an occupant similar to AM50, although further study is needed to investigate the variability in the muscle activity among the same size of drivers as AM50.

Activation levels of the muscles predicted by the musculoskeletal model were used as inputs for the muscle models of the human FE model with the body size of AM50 in bracing. However, in order to apply the predicted activation level of each muscle to the corresponding muscle of the human FE model, the human FE model should be comparable in shapes and sizes of the bones, muscle attachments to the bones, and joint properties with the musculoskeletal model. The musculoskeletal model was developed based on the skeletal geometry of the human FE model and the muscle attachments to the bones were duplicated in the human FE model. Although body size and weight of the subject used in the volunteer test was similar to those of the human FE model, in particular, the length of skeletal parts in the lower extremity was a little bit different between the subject and the human FE model. Therefore, the musculoskeletal model was modified to fit the subject's anthropometric data before predicting muscle activation levels and then the activation levels were adjusted to fit the human FE model using some scaling techniques. The hip and knee joints were modeled using a rotational joint with reasonable material properties and the ankle joint was modeled as bone-to-bone contacts with major ligaments in the human FE model while all joints of the lower

extremity in the musculoskeletal model were modeled using a similar type of rotational joint as used in the human FE model. However, the ankle joint was validated against test data on dorsiflexion/plantarflexion and inversion/eversion of human surrogates (Iwamoto et al., 2000). In addition, extensor muscle of soleus attached to the Achilles tendon provided muscular force of 1.9 kN in the parametric simulations with activated muscles (Figure 9). Some researchers provided human subjects with 1.0 to 2.6 kN of Achilles tendon forces in their experimental cadaver tests based on their preliminary study in order to investigate the muscular effect for the lower leg skeletal injuries (e.g. Funk et al., 2001 and Kitagawa et al., 1998). This indicates that the activation levels predicted by the musculoskeletal model were quite reasonable. Thus, the activation levels predicted by the musculoskeletal model can be used to reproduce muscle activation levels of the human FE model when pressing the pedal.

In this study, we assumed that the human body was impacted from the foot by a brake pedal when the muscle activation levels showed maximal voluntary contraction in order to investigate effect of muscle tense on lower leg skeletal injuries caused by the intrusion in frontal impacts. To reproduce the pre-impact situation, the reaction force from the seat bottom was applied to the buttock and right and left thighs. As shown in Figure 7, the simulation result is comparable in pressure distribution and contact force to experimental test. Therefore, the pre-impact situation was reproduced by using the human FE model.

Pedal forces predicted by the FE simulation were comparable to emergency braking forces using driving simulators obtained from the literature (Owen et al. 1998 and Yoshida et al. 1998). Therefore, the predicted pedal forces might reproduce those obtained from emergency braking situation. Parametric simulations on the pedal impacts to the foot demonstrated that there were significant difference in peak compressive forces at the tibia according to the pre-impact conditions on the muscles. The peak force in the condition with activated muscle was significantly greater than that with relaxed muscle. As shown in Figure 9, the extensor muscles at the knee and hip joints were predominantly activated in the pedal impact simulations with activated muscles. This indicates that the extension of the knee and hip joints and the pedal intrusion prevented the knee from coming upward. Therefore, activated muscles in the hip and right thigh kept the tibia fixed, and as a result, they increased the axial compressive force in the activated case. The peak force in the condition with relaxed muscle was a little bit greater than that without any muscles. This result suggests that passive muscular property contributed to the increase of the tibial axial force.

This study employed two injury criteria of a plastic strain based criterion and the RTI to investigate the possibility of bone fractures in the tibia. The plastic strains appeared at both the distal tibia and tibial diaphysis in the case with activated muscles while the strains appeared only at the distal tibia with relaxed muscles. The RTI also estimated 50% probability of AIS 2+ leg injury at the diaphysis with activated muscles while it did not estimate 25% probability of AIS 2+ leg injury at both the diaphysis and the distal end with relaxed cases. The reason why activated muscle case had the possibility of bone fractures at the diaphysis is because a bending moment was applied to the tibia due to preventing the knee from moving upward. The investigation by using two injury criteria suggested that the activated muscles of the lower extremity could increase the possibility of tibial fractures.

Many researchers conducted cadaver tests on the impacts for the foot with an assumed Achilles tendon force to reproduce the axial impact for the tibia with a fixation of the proximal tibia, which simulated an entrapped knee observed in automotive frontal crashes (e.g. Funk et al., 2001 and Kitagawa et al., 1998). They found bone fractures, in particular, at the tibia, fibula, talus, and calcaneus and concluded that the muscular tension force at the Achilles tendon could increase bone fractures in those bones. Some studies using human FE model also provided the same conclusion (e.g. Iwamoto et al., 2005 and Kitagawa et al., 1998). In this study, as mentioned above, parametric simulations without the entrapped knee indicated that activated muscles in the hip and right thigh played a similar role in the entrapped knee and then activated crural muscles could increase tibial compressive force and possibility of bone fractures at the tibia. According to cadaver tests conducted by Klopp et al. (1995) and Levine et al. (1978), the activated thigh muscles tend to prevent the knee from moving forward and keep the knee fixed during frontal collisions. This supports that the activated muscles in the hip and right thigh cause the entrapped knee in frontal collisions.

LIMITATIONS OF THIS STUDY: There are some limitations on modeling the muscles in the occupant FE models used in this study. First of all, each muscle of the right lower extremity in the occupant FE model was modeled using bar elements and attached to bones by merging nodes between the muscles and the bones. Therefore, activated muscular force could cause stress concentrations to generate bone fractures at the muscle attachments. This study avoided the stress concentrations by representing the elements of bones attached to the muscle as rigid bodies. However, this method can not be used to evaluate bone fractures at the muscle attachments, although it can be used for bone fracture predictions at the distal tibia and tibial diaphysis because the middle and distal parts of the tibia have little muscle attachments. Secondly, via-points of each muscle cannot move in this study, although actual muscles can slide on the bones according to motions of the human body. Thirdly, the transverse stiffness of each muscle is the same between activated state and relaxed state, because the bar elements cannot reproduce the stiffness change in the transverse direction. In addition, the activation levels were given as constant ones from a driver's maximum voluntary contraction during the impact simulations. This is because muscle responses for an emergency braking in real-world accidents are still unknown and the individual variability in muscle activation among the same size of drivers is not adequately investigated yet. Furthermore, the current musculoskeletal model does not include muscles of upper bodies. Consequently, the model cannot be used for investigation on effect of muscle tense in upper extremities and trunk to upper body injuries. Finally, the parametric simulations performed in this study did not represent inertia effects caused by deceleration during impacts. Since occupants can move forward due to the inertia effects, the axial compressive force at the tibia can increase more significantly than without the inertia effects. However, as Klopp et al. (1995) and Levine et al. (1978) suggest that activated thigh muscles could prevent the occupants from moving forward, further study is needed to investigate if the thigh muscles are effective to prevent the submarining or they increase the possibility of bone fractures at the tibia.

CONCLUSIONS

This study investigates effects of muscle tense in bracing on impact responses and skeletal injuries of a driver's lower extremity in a simulated frontal crash situation with pedal intrusion. An experimental volunteer test using a male subject with the same size as AM50 was conducted to obtain some measurements of EMG, pedal force, and pressure distributions of a seat bottom and a seat back in his maximum voluntary contraction. Based on the experimental test data, muscle activation levels in bracing were predicted by inverse dynamics analysis using a musculoskeletal model with 33 skeletal muscles of the right lower extremity not only in superficial layer but also in deep layer. The activation levels of the musculoskeletal model were used as those of an AM50 occupant FE model to simulate driver's bracing. Parametric studies on the pedal impacts to the foot were performed using the occupant FE model with three pre-impact muscular conditions to investigate the effects of muscle tense on the lower leg skeletal injuries. Simulation results reveal that activated thigh muscles could cause the entrapped knee in frontal collisions and therefore the activated crural muscles could increase axial compressive force and possibility of bone fractures at the tibia. However, there are still some limitations on modeling the muscles in occupant FE models. Further study is needed to improve stress concentration at muscle attachments and to control via-points in each muscle. Additionally, the simulation setup used in this study only represents an assumed impact situation without inertia effects in frontal crashes. Therefore, additional simulations are necessary to elucidate injury mechanisms of the lower leg with considering effect of the inertia force. Future works include prediction of muscle activation levels for the upper extremities during pressing a steering wheel or holding it and investigation of the muscular effects for the skeletal injuries of the upper body.

ACKNOWLEDGMENTS

The authors would like to acknowledge Toyota Technical Development Corporation for their supports in developing the human FE model. We also wish to thank NAC Image Technology, Inc. in Japan for their technical supports of motion analysis.

REFERENCES:

- (1) Begeman, P., King, A.I., Levine, R., Viano, D.C., (1980), Biodynamic Response of the Musculoskeletal System to Impact Acceleration. Proc. of the 24th Stapp Car Crash Conference,

- SAE Paper No. 801312, pp. 479-509.
- (2) Behr, M., Arnoux, P.-J., Serre, T., Thollon, L., Brunet, C., (2006), Tonic Finite Element Model of the Lower Limb, *Journal of Biomechanical Engineering*, Vol. 128, pp.223-228.
 - (3) Buford, W.L., Ivey, M., Marone, J.D., Patterson, R.M., Peare, G.L., Nguyen, D.K., Stewart, A.A., (1997) Muscle balance at the knee-moment arms for the normal knee and the ACL-Minus knee, *IEEE Transactions on Rehabilitation Engineering*, Vol. 5, No. 4, pp. 367-379.
 - (4) Camacho, D.L., Nightingale, R.W., Robinette, J.J., Vanguri, S.K., Coates, D.J., and Myers, B.S. (1997) Experimental flexibility measurements for the development of a computational head-neck model validated for near-vertex head impact. *Proc. 41st Stapp Car Crash Conference*, SAE Paper No. 973345.
 - (5) Choi, H.Y., Sah, S.J., Lee, B., Cho, H.S., Kang, S.J., Mun, M.S., Lee, I., and Lee, J., (2005), Experimental and numerical studies of muscular activations of bracing occupant. Paper No. 05-0139-O, *Proc. of 19th International Technical Conference on the Enhanced Safety of Vehicles (ESV)*, Washington DC.
 - (6) Crandall, J.R., Portier, L., Petit, P., Hall, G.W., Bass, C.R., Klopp, G.S., Hurwitz, S., Pilkey, W.D., Trosseille, X., Tarrière, C., and Lassau, J. (1996), Biomechanical Response and Physical Properties of the Leg, Foot, and Ankle. *Proc. of the 40th Stapp Car Crash Conference*, pp. 173-192. Society of Automotive Engineers, Warrendale, PA.
 - (7) Funk J.R., Crandall J.R., Tourret L.J., MacMahon C.B., Bass C.R., Khaewpong N.K., Rppinger R.H., (2001), The effect of active muscle tension on the axial injury tolerance of the human foot/ankle complex. *Proc. 21st ESV Conference*, Paper No. 237, pp. 1-14.
 - (8) Gans, C. (1982), Fiber architecture and muscle function. *Exercise and Sports Sciences Reviews*. 10, pp. 106-107.
 - (9) Griffin, B.N., (1978), *Design Guide: The Influence of Zero-G and Acceleration on the Human Factors of Spacecraft Design*, NASA Johnson Space Center.
 - (10) Hada M., Yamada, D., and Tsuji, T., (2007), An Analysis of Equivalent Impedance Characteristics by modeling the Human Musculoskeletal Structure as a Multibody System. *Proc. of An ECCOMAS Thematic Conference on Multibody Dynamics*, Milano, 25-28 June (in press).
 - (11) Iwamoto, M., Tamura, A., Furuu, K., Kato, C., Miki, K., Hasegawa, J., Yang, K.H., (2000), Development of a Finite Element Model of the Human Lower Extremity for Analyses of Automotive Crash Injuries, *SAE Trans. J. of Passenger Car, Mech.Sys.*, 109(6), pp.846-853.
 - (12) Iwamoto, M., Kisanuki Y., Watanabe I., Furuu K., Miki K., Hasegawa J., (2002), Development of a Finite Element Model of the Total Human Model for Safety (THUMS) and Application to Injury Reconstruction. *Proc., International Research Council on the Biomechanics of Impact*, Munich, Germany, pp. 31-42.
 - (13) Iwamoto, M., Miki, K., Tanaka, E., (2005), Ankle Skeletal Injury Predictions Using Anisotropic Inelastic Constitutive Model of Cortical Bone Taking into Account Damage Evolution. *Proc. 49st Stapp Car Crash Conference*, SAE Paper No. 05S-24.
 - (14) Kitagawa, Y., Ichikawa, H., King, A.I., and Levine, R.S., (1998), A severe ankle and foot injury in frontal crashes and its mechanism. *Proc. of the 42nd Stapp Car Crash Conference*, SAE Paper No. 983145, Society of Automotive Engineers, Warrendale, PA.
 - (15) Klopp G.S., Crandall J.R., Sieveka E.M., Pilkey W.D., (1995), Simulation of muscle tensing in pre-impact bracing. *IRCOBI conference 1995*, pp.171-182.
 - (16) Kuppa S., Wang J., Haffner M., Eppinger R., (2001), Lower extremity injuries and associated injury criteria. *Proc. of 17th International Technical Conference on the Enhanced Safety of Vehicles (ESV)*, Amsterdam, Netherlands.
 - (17) Levine R.S., Patrick L.M., Begeman P.C., King A.I., (1978), Effect of quadriceps function on submarining. *Proc. of the 22th Conference of Association for the Advancement of Automotive Medicine (AAAM)*, pp. 319-329.
 - (18) Lloyd D.G. and Besier T.F., (2003) An EMG-driven musculoskeletal model to estimate muscle forces and knee joint moments in vivo., *J. Biomech.*, 36, pp.765-776.
 - (19) Morgan, R.M., Eppinger, R.H., Hennessey, B.C., (1991), Ankle Joint Injury Mechanism for Adults in Frontal Automotive Impact. *Proc. of the 35nd Stapp Car Crash Conference*, SAE Paper No. 912902, pp. 189-198.

- (20) Owen, C., Roberts, A., Manning, P., Lowne, R., (1998), Positioning and bracing of the lower leg during emergency braking – A volunteer study., IRCOBI conference 1998, pp. 147-159.
- (21) Spoor C.W., Leeuwen, J.L., Meskers, C.G., Titulaer, A.F., Huson, A., (1990), Estimation of instantaneous moment arms of lower-leg muscles, J.Biomech. Vol. 23, No. 12, pp. 1247-1259.
- (22) States, J.D., (1986), Adult Occupant Injuries to the Lower Limb. SAE Paper No. 861927, pp.97-107.
- (23) Tennyson S.A., King A.I., (1976), A Biodynamic Model of the Human Spinal Column. SAE Paper No. 760771.
- (24) Winters, J.M. (1990) 'Hill-Based Muscle Models: A System Engineering Perspective', in Multiple Muscle Systems: Biomechanics and Movement Organization, Winters, J.M. and Woo. S. (eds.), New York, Springer, pp. 66-93.
- (25) Winters, J.M. Woo. S. (1990), Multiple Muscle Systems: Biomechanics and Movement Organization, New York, Springer, pp. 726-749.
- (26) Yamada, H., (1970), Strength of Biological Materials, Williams & Wilkins Company.
- (27) Yamada, D., Hada, M., (2007), An Estimation Method of Muscle Force by Variable Moment Arm Vector, SAE Digital Human Modeling for Design and Engineering Conference and Exhibition, Seattle, Washington DC., SAE Paper No. 2007-01-2468.
- (28) Yoshida, H., Sugitani, T., Ohta, M., (1998), Development of the brake assist system, International congress and exposition, Detroit, Michigan, SAE Paper No., 980601.